Journal of Civil Engineering and Urban Planning (2023)
Clausius Scientific Press, Canada
DOI: 10.23977/jceup.2023.050409
ISSN 2616-3969 Vol. 5 Num. 4

Reliability Analysis of Post-fire RC Beams Strengthened with CFRP

Ansheng Wu[1,*], Yanwei Hou[2]

[1]*School of Road and Bridge & Architectural Engineering, Shaanxi Railway Institute, Weinan, 714000, China*
[2]*School of Art, Shangqiu University, Shangqiu, 476000, China*
[*]*Corresponding author*

Keywords: Reinforced concrete, CFRP, Post-fire, Monte Carlo method, Reliability

Abstract: In order to study the variation law of flexural capacity reliability of reinforced concrete (RC) beams exposed to high temperature, a calculation method for flexural capacity of RC beams after fire was proposed based on the improved section method. The mechanical properties of post-fire RC beams were tested. The temperature field distribution of RC beams after fire was numerically simulated and verified by ABAQUS, and the reliability analysis of post-fire RC beams strengthened with Carbon Fiber Reinforced Polymer (CFRP) was carried out by Monte Carlo method. The calculation results show that with the increase of load ratio and fire time, the reliability of the flexural capacity of RC beams after fire decreases obviously, but with the increase of the number of layers of CFRP sheets, the reliability of the flexural capacity of RC beams after fire increases obviously, and the reliability improvement effect is most significant when two layers CFRP sheets are reinforced. The analysis results can provide a reference for the subsequent research on mechanical properties of post-fire reinforced concrete structures reinforced by CFRP.

1. Introduction

Fire hazards seriously endanger human life and property safety, while building fire accounts for a large proportion in all fires in the world, so it has always become the focus of domestic and foreign scholars [1]. In a building fire, the reinforced concrete (RC) beam is located at the upper part of building structure, the temperature is the highest, so it suffers the most serious fire damage [2].

The reinforced concrete beam is affected by the high temperature of fire, resulting in the reduction of mechanical properties such as the elastic modulus and strength of the concrete and the steel bars of the structure, so that the bearing capacity of the RC structure may not meet the initial design requirements [3]. Therefore, it is of great importance to study the residual bearing capacity of reinforced concrete structure after fire.

At present, scholars have studied the bearing capacity of reinforced concrete beams after fire. In 2013, Xu and Wu conducted static tests on seven RC beams after high temperature and three contrast beams at normal temperature, and conducted experimental research on the residual bearing performance of beams, and proposed a practical calculation formula for the shear capacity of reinforced concrete beams subjected to fire on three sides [4]. Li and Tang finished fire tests on 11 reinforced concrete simply supported beams on three sides and conducted an in-depth study on the flexural performance and reliability of the specimens [5].

Although there are many studies on the residual bearing capacity of reinforced concrete beams after fire, there are still few tests and finite element analysis on the flexural bearing capacity of reinforced concrete beams after fire. In particular, there are limited studies on the fitting between the internal temperature field of a member after fire and the simulated temperature field by finite element, which results in the decrease of the accuracy on the simulated temperature field of a member after fire.

The strengthening of reinforced concrete structures after fire has become the main research topic in structural area. Through the theory and practical cases, it is proved that adopting the reasonable method to strengthen the concrete structure has a remarkable effect on improving the bearing capacity of the structure and prolonging the service life of the structure. Structural reinforcement technology not only improves the safety degree in the use of structures, but also earns a large number of social and economic benefits, bringing a lot of income for the construction of social infrastructure [6].

The reinforcement methods of reinforced concrete structures are classified into direct reinforcement and indirect reinforcement [7]. Among the indirect reinforcement technologies, fiber reinforced plastic (FRP) reinforcement technology has developed most rapidly. It is widely used in construction engineering fields worldwide due to its extremely high corrosion resistance and wear resistance, as well as high strength characteristics. FRP material includes carbon fiber reinforced polymer (CFRP), glass fiber reinforced materials (GFRP) and arylon fiber reinforced materials (AFRP), etc. Up to now, carbon fiber external bonding method has been a more common reinforcement method [8]. There is a lack of research on the reliability of the bearing capacity of CFRP reinforced concrete structures after fire at home and abroad. Therefore, the research on the reliability index of post-fire reinforced concrete structures has important practical application value and theoretical research significance.

A total of four reinforced concrete beams are designed, among which two beams are subjected to fire test and two beams in the contrast group are without high-temperature treatment. The temperature field is analyzed and the influence of fire time on the ultimate bearing capacity is studied. In order to reduce the variability of test data caused by component defects and ensure the reliability of test data, two beams are used under each condition in the test. After the fire tests of reinforced concrete beams, the reduction of mechanical performance of concrete and reinforcements is studied and the fire resistance of the beam is further analyzed. Through the bending loading test of the RC beams after the fire treatment, the correctness of the finite element simulation method is analyzed and verified, and then the CFRP-reinforced beams after fire is studied. The calculation method of structural reliability is applied, the MATLAB [9] calculation software is adopted, and Monte Carlo method is used to carry out the reliability analysis of reinforced concrete beams reinforced by CFRP after fire.

2. Test Overview

2.1. Specimen Design

In the experiment, the influence of fire time on reinforced concrete beams is considered, the commonly used three-side fire is adopted. A total of four beams is divided into two groups, experimental group (L3, L4) and control group (L1, L2). The sectional size of beams is $b \times h = 120\text{mm} \times 150\text{mm}$. The lower tensile steel bar is HRB400 with diameter of 12 mm, and the upper compressive steel bar is 10 mm. The thermocouple installation holes are reserved with diameter of 20 mm. 20 standard concrete test blocks are poured in the same batch of concrete, and the standard test blocks are used to test the axial compressive strength of concrete. Figure 1.

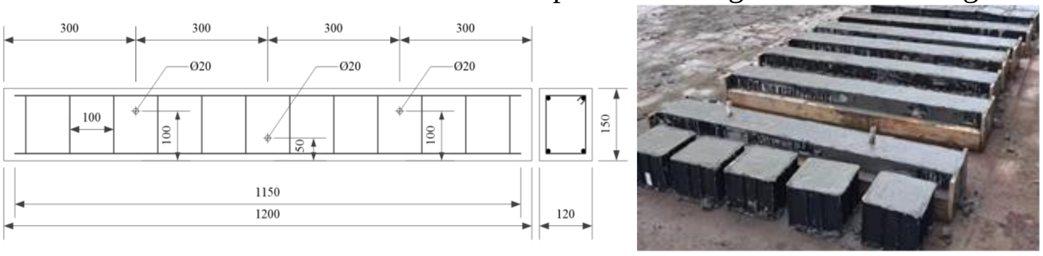

(a)Dimensions diagram (b) Specimen photograph

Figure 1: Dimensions of reinforced concrete beams

The C30 commercial concrete is adopted, which is prepared by 42.5 grade ordinary Portland cement, with water-cement ratio of 0.47, medium coarse sand, with sand rate of 0.4, gravel with diameter of 5~25 mm. Table 1.

Table 1: Mix proportion of concrete.

component	water	ordinary Portland cement	sand	stone
proportion	0.38	1	1.11	2.72
mass(kg)	175	461	512	0.3

In the process of fabrication, the reinforcements are bound according to the design size of specimen, and the template is made. Before pouring, PVC pipe is inserted into the marked point inside the reinforcement cage, and is extracted after the initial setting of concrete, so as to reserve the measuring points of thermocouple elements for the subsequent fire test of reinforced concrete beam. After casting, the concrete is vibrated and compacted, kept at room temperature (22°C) for 24 h, demudded and cured at room temperature with relative humidity of 95%±5%, and maintained curing until 28 days.

The temperature measuring element adopted K-type thermocouple with the model of RH-8000A. The layout of thermocouples for specimens L3 and L4 is arranged according to Figure 2. After inserting to measuring points, the thermocouples are bound and fixed with heat-resistant wire, cement slurry is poured and fire-proof cotton is laid for fire test.

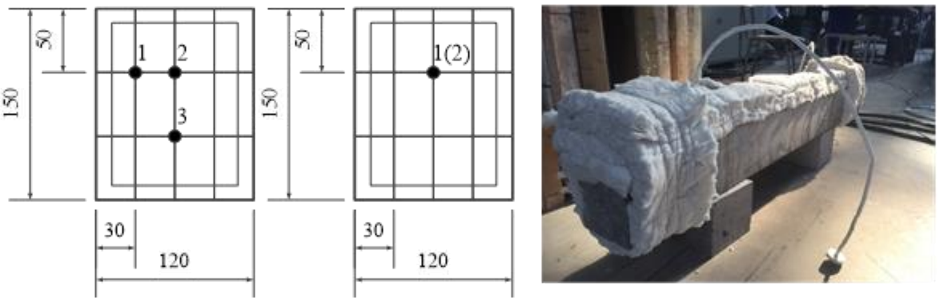

Figure 2: Layout of thermocouple for reinforced concrete beams.

2.2. Fire Test and Temperature Acquisition

In order to reduce the variation of test data, fire test is carried through on two RC beams first, Maintain high temperature for 60 minutes. Five standard concrete test blocks are used for the same condition test, so as to obtain the reduction data of concrete.

The test was divided into two phases, the fire test equipment is rectangular combined fire test furnace, the temperature limit of the test furnace is 1200℃, and the maximum power is 21 kW, which is shown in Figure 3(a), the flexural capacity loading equipment is tested by a 50-ton hydraulic press, as seen in Figure 3(b).

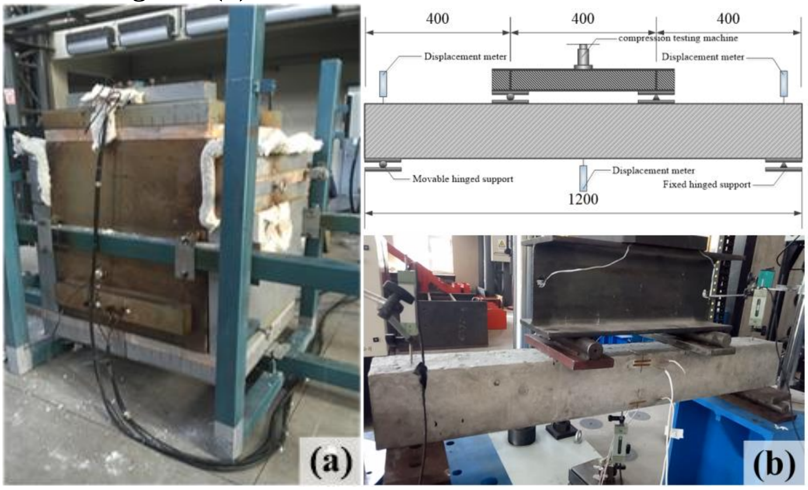

Figure 3: Test equipment. (a) Fire equipment (b) Loading equipment

Figure 4 shows the curve of temperature rising time t (min) in the furnace versus temperature T (℃) in the furnace during the fire test of reinforced concrete beams, which is compared with ISO-834 international standard temperature rise curve. The formula of temperature rise curve is:

$$T = T_0 + 345\lg(8t+1) \tag{1}$$

T_0 is the indoor temperature under actual simulation or test state, t is the fire heating time.

In Figure 4, due to the factors such as slow electric heating, the tightness of fire furnace, and the incomplete operation of the electric heating wire on account of the use loss, After 10 minutes, the temperature curve is consistent.

Figure 4 also shows the measured curve of each measuring point of the thermocouple in the fire test for specimens L3 and L4. The fire time is 60 min. It can be clearly seen from the specimens that the surface of the unexposed concrete wrapped by fireproof cotton at both ends of the beam does not change, while the fire surface of concrete becomes gray and white after the fire test, and there are fine cracks on the surface.

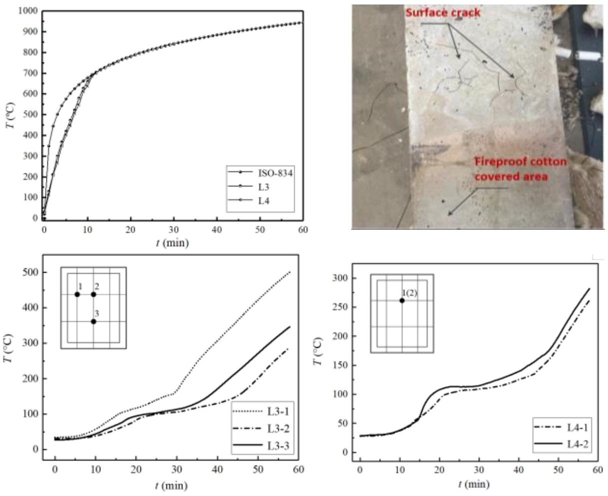

Figure 4: Temperature curves of fire furnace and each measuring point.

2.3. Flexural Test and Test Results

Figure 5 shows the load-deflection curves of L1-L4, which records the results during the loading process of specimens L1 and L2 until the specimens in the mid-span compression zone is crushed and declared to be destroyed. When the mid-span deflection of specimen L1 reaches 9.83 mm, the peak load reaches 73.01 kN. When the mid-span deflection of specimen L2 reaches 9.97 mm, the peak load reaches 75.12 kN.

Figure 5(c) and 5(d) show the load-deflection curves of specimens L3 and L4 obtained by the flexural test after 1 hour. When the mid-span deflection of specimen L3 reaches 10.94 mm, the peak load reaches 54.96 kN. When the mid-span deflection of specimen L4 reaches 10.65 mm, the peak load reaches 47.88 kN.

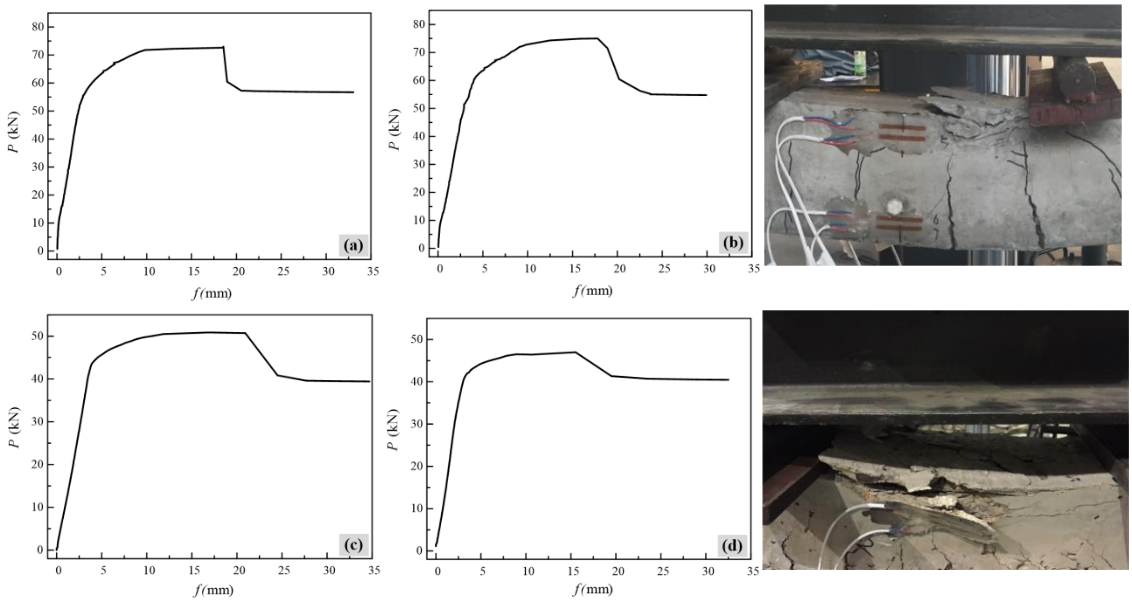

Figure 5: Load-deflection curves. (a) L1 (b) L2 (c)L3 (d)L4

Table 2: Bearing capacity results of specimens.

specification	dimension(mm)	fire time(min)	yeild load (kN)	mid-span deflection at failure(mm)
L1	120×150	0	63.21	4.83
L2	120×150	0	61.12	4.78
L3	120×150	60	43.74	4.01
L4	120×150	60	41.02	3.83

According to the data in Table 2. Compared with specimens unexposed to fire, when the fire time reaches 60 min, the bearing capacity of the specimens decreases by 25.79%, which shows that the high temperature causes great damage to the concrete material.

3. Finite Element Simulation and Calculation for Bearing Capacity

3.1. Thermal Parameter

The main parameters of thermodynamic properties of materials are the basis for calculating the temperature distribution of components. The thermal models proposed by EC4 [10] are adopted for steel bars and ordinary concrete.

The specific heat capacity of concrete, C_c:

$$c_c = 900 - 4(\frac{T}{120})^2 + 80(\frac{T}{120}) \qquad 20℃ \le T \le 1200℃ \tag{2}$$

The heat conductivity of concrete, λ_c:

$$\lambda_c = 2 - 0.24(\frac{T}{120}) + 0.012(\frac{T}{120})^2 \qquad 20℃ < T \le 1200℃ \tag{3}$$

The thermal expansion coefficient of concrete refers to the formula summarized by Lie [11], is given as:

$$(\frac{\Delta l}{l})_c = (0.008T + 6) \times 10^{-6} \tag{4}$$

The thermal expansion coefficient of steel bars refers to European standard [12], is given as:

$$\alpha_s = 1.4 \times 10^{-5} \qquad 20℃ \le T \le 1200℃ \tag{5}$$

The specific heat capacity of the steel bars refers to European standards EC3 and EC4 [12], is given as:

$$\lambda_s = 54 - 3.33 \times 10^{-2} T \qquad 20℃ \le T \le 800℃ \tag{6}$$

$$\lambda_s = 27.3 \qquad 800℃ < T \le 1200℃ \tag{7}$$

3.2. Temperature Field Simulation and Verification

In the fire process of reinforced concrete member, small cracks will be generated on the outer surface of member at high temperature, and heat will penetrate into the structure from the cracks, leading to local high temperature of member and local variation of temperature field. Temperature redistribution variation and high temperature caused by cracks are ignored in the research process, and tie contact is adopted between reinforcement and concrete in simulation.

In order to verify the accuracy of the thermal parameters used in the finite element simulation and the correctness of the selection of various thermal parameters and interface definition methods, the finite element simulation is carried out, and the temperature nephogram is obtained and the simulated temperature curve is compared with the measured temperature curve of the thermocouple in the fire test, Figure 6.

It can be seen that when the temperature reaches 100°C, the growth trend of the measured temperature curve slows down due to the evaporation of water, which is slightly different from the simulated curve. However, the temperature growth trend of the two curves is basically the same gradually, and the fitting effect is well. In conclusion, the thermal parameters and theoretical analysis used in the finite element simulation by ABAQUS are reasonable and effective, and the establishment of the temperature field model and the calculation process are correct.

3.3. Bearing Capacity Simulation Verification

The finite element model of RC beams is established the previous temperature field analysis, and theoretical calculation is conducted. The calculated bearing capacity are compared with the experimental values and simulated values to verify the correctness and reliability of the finite element simulation calculation method.

Thermodynamic properties of steel

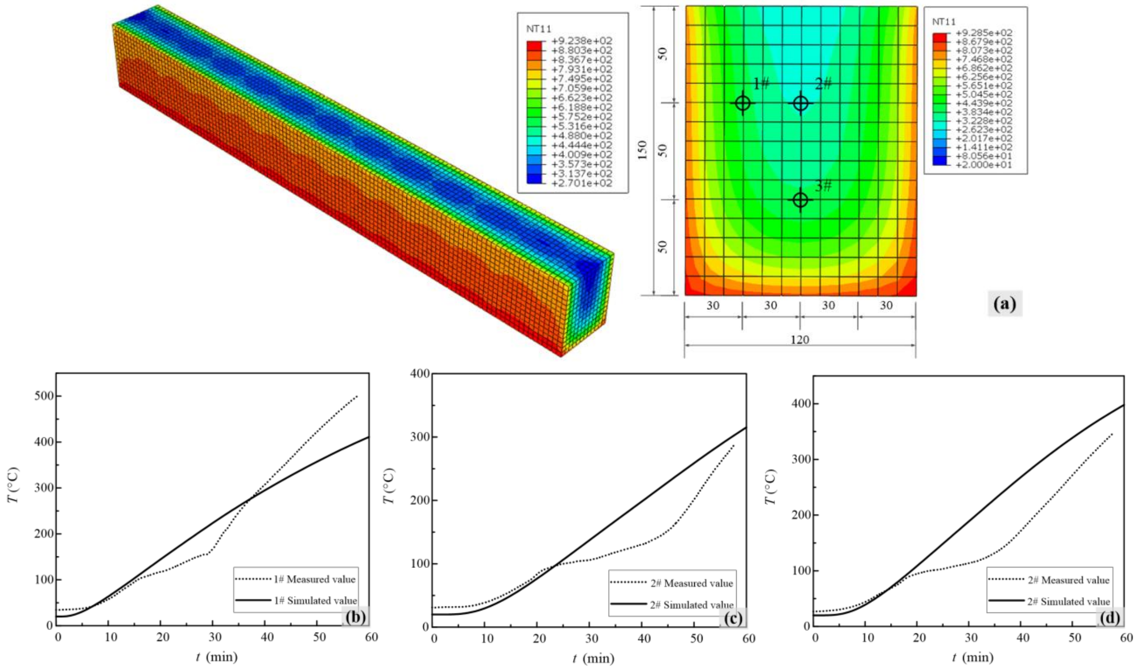

Figure 6: Simulated temp nephogram and comparison with measured temperature in test after heating for 60 min.

The stress-strain relationship of steel bars at high temperature adopts the stress-strain relationship model proposed by Lie [13], is given as:

$$\sigma_s = \begin{cases} \dfrac{f(T,0.001)}{0.001}\varepsilon_s & \varepsilon_s \le \varepsilon_p \\ \dfrac{f(T,0.001)}{0.001}\varepsilon_p + f\left[T,(\varepsilon_s - \varepsilon_p + 0.001)\right] - f(T,0.001) & \varepsilon_s > \varepsilon_p \end{cases} \tag{8}$$

Elastic modulus formula at high temperature is given as:

$$E_{sh}(T) = \frac{f(T,0.001)}{0.001} = (50000 - 40T) \times \left\{1 - \exp\left[(-30 + 0.03T)\sqrt{0.001}\right]\right\} \times 6.9 \tag{9}$$

Yield strength at high temperature is given as:

$$f_{yh}(T) = \frac{f(T,0.001)}{0.001}\varepsilon_{yh} = 4\times10^{-3} f(T,0.001) f_y \tag{10}$$

$$\varepsilon_{yh}(T) = \varepsilon_p = 4\times10^{-6} f_y \tag{11}$$

The μ_s is 0.283.

Thermodynamic properties of concrete

Stress-strain relationship of concrete at high temperature is given as:

$$\frac{\sigma_c}{f_c'(T)} = \begin{cases} 1 - \left[\dfrac{\varepsilon_p(T) - \varepsilon_c}{\varepsilon_p(T)}\right]^2 & \varepsilon \le \varepsilon_p \\ 1 - \left[\dfrac{\varepsilon_p(T) - \varepsilon_c}{3\varepsilon_p(T)}\right]^2 & \varepsilon > \varepsilon_p \end{cases} \tag{12}$$

The elastic modulus of concrete at high temperature adopts the formula proposed by Lu [14]:

$$\frac{E_{cT}}{E_c}=\begin{cases}1-0.0015T & 0^{\circ}C<T\le 200^{\circ}C\\ 0.87-0.00084T & 200^{\circ}C<T\le 700^{\circ}C\\ 0.28 & 700^{\circ}C<T\le 800^{\circ}C\end{cases} \tag{13}$$

Where E_c is elastic modulus of concrete at room temperature, $E_c=4730\sqrt{f_c'}$

The Poisson's ratio of concrete at high temperature calculation adopts the formula proposed by Germay [15], is given as:

$$V(T)=\begin{cases}V\left(0.2+0.8\dfrac{500-T}{480}\right) & T\le 500^{\circ}C\\ 0.2V & T>500^{\circ}C\end{cases} \tag{14}$$

The V is 0.2.

After the simulated values are compared with the test values. The load-deflection curves of specimens L1 and L2 are compared with the model without fire exposure, Figure 7(a), and the load-deflection curves of specimens L3 and L4 are compared with the model for 60 minutes of fire exposure. Figure 7(b), the deflection at yield and the load in ultimate state are basically the same, the simulated results fit well with the experimental values.

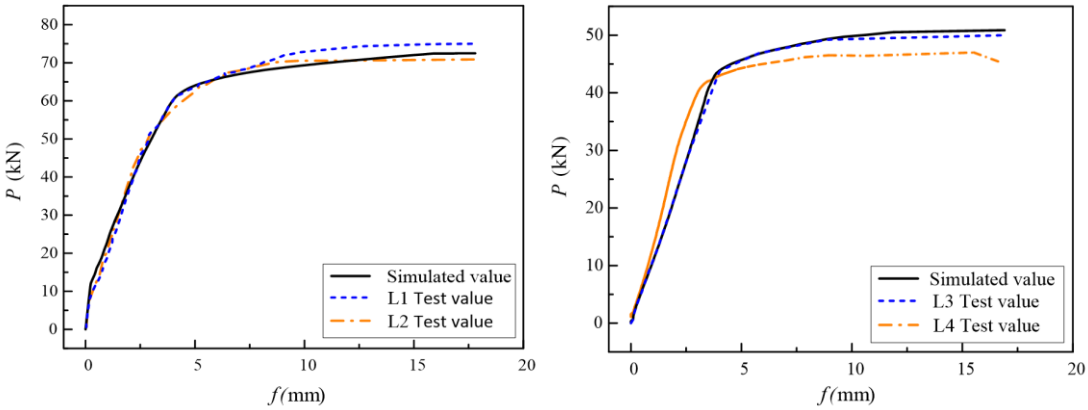

Figure 7: Comparison of load-deflection curves of specimens. (a)L1, L2 (b)L3, L4

3.4. Calculation Formula of Flexural Capacity

The residual compressive strength of concrete after fire adopts the formula in literature [16], is given as:

$$\varphi_{CT}=\frac{f_{cr}(T)}{f_c}=\begin{cases}1.0 & 0℃<T\le 200℃\\ \left[1.0-0.0015(T-200)\right] & 200℃<T\le 500℃\\ \left[0.25+0.003(600-T)\right] & 500℃<T\le 600℃\\ \left[0.25-7.5\times10^{-4}(T-600)\right] & 600℃<T\le 800℃\end{cases} \tag{15}$$

φ_{CT} is reduction coefficient of compressive strength of concrete after fire.

The Poisson's ratio of concrete at high temperature calculation adopts the formula proposed by Germay [15], is given as:

The reduction coefficient of residual strength of steel bars after fire proposed by Shen [17] is given as:

$$\varphi_{yT}=\frac{f_{yr}(T)}{f_y}=\begin{cases}(99.838-0.0156T)\times10^{-2} & 0℃<T<600℃\\ (137.35-0.0754T)\times10^{-2} & 600℃\le T\le 900℃\end{cases} \tag{16}$$

Where $f_{yr}(T)$ is yield strength of steel bars at temperature T.

The bearing capacity of reinforced concrete beams after fire is given as:

$$M_{CT} = \alpha_1 \bar{\varphi}_{CT} f_c bx(h_0 - 0.5x) + \varphi'_{yT} f'_y A'_s (h_0 - a'_s) \tag{17}$$

$$\alpha_1 \bar{\varphi}_{CT} f_c bx = \varphi_{yT} f_y A_s - \varphi'_{yT} f'_y A'_s \tag{18}$$

where b is beam width, h_0 is beam effective height, x is the height of compression zone after fire, $A_{s'}$ is sectional area of reinforcements in compression zone, α_1 is a factor, when the concrete strength grade does not exceed C50, α_1 is taken as 1, $\bar{\varphi}_{CT}$ is reduction coefficient of average compressive strength of concrete after fire, φ_{yT} is strength reduction coefficient of tensile reinforcements after fire,.

The flexural capacity and yield load of reinforced concrete beams are calculated by the actual measured values of materials in test. The numerical values obtained by finite element simulation are summarized and compared with test results, as shown in Table 3. The strength reduction coefficients of concrete in compression zone and reinforcements after fire are calculated, and the theoretical calculation values of yield load and flexural capacity are obtained. It verifies that the finite element method is accurate and effective in calculating the bearing capacity of reinforced concrete beams before and after fire, which can provide basis and reference for future experimental research.

Table 3: Comparison of bearing capacity of reinforced concrete beams.

specification	test values		simulated values		calculated values	
	Load (kN)	Moment (MPa)	Load (kN)	Moment (MPa)	Load (kN)	Moment (MPa)
L1	63.21	12.64	63.22	12.64	62.30	12.46
L2	61.12	12.22				
L3	43.74	8.75	43.83	8.77	44.75	8.95
L4	41.02	8.20				

4. Finite Element Simulation and Calculation for Bearing Capacity

A new model is established by the obtained thermal parameters, and the bearing capacity is analyzed after the fire treatment. After CFRP reinforcement, Monte Carlo (MC) method is used to calculate the component reliability index by MATLAB software.

4.1. Load Determination and Load Statistical Parameters

The load of the beam is determined before reinforcement, which composes of normal live load q_{1Q}, dead weight load of beam plate q_{1G} ,and dead weight load of ceiling decoration q_{2G}, so the bending moment generated by the live load applied to the component , M_Q , is given as:

$$M_Q = \frac{1}{8} q_{1Q} l^2 \tag{19}$$

The model is established by the obtained thermal parameters, and the bearing capacity is analyzed after the fire treatment. After CFRP reinforcement, MC method is used to obtain component reliability index by MATLAB software.

Where l is member length.

The bending moment generated by the dead load is:

$$M_G = \frac{1}{8}(q_{1G} + q_{2G}) l^2 \tag{20}$$

When determining the bending load for a component, the most unfavourable factors should be considered, that is, the maximum sectional M controlled by the dead load or the maximum sectional M controlled by the live load should be taken as the design bending moment in load effect combination.

$$M_{sd} = \max\left\{\left(\xi\gamma_G M_G + \gamma_Q M_Q\right);\left(\gamma_G M_G + \gamma_Q \psi_c M_Q\right)\right\} \tag{21}$$

Where ξ is the reduction coefficient of constant load controlled by live load, γ_G is partial coefficient of dead load, γ_Q is partial coefficient of live load, ψ_c is adjustment coefficient for combined value of live load.

The specific statistical parameters for dead and live loads are shown in Table 4:

Table 4: Statistical parameters of load.

random parameter	mean value/ standard value	standard deviation	coefficient of variation	distribution type
dead load	1.060	0.074	0.070	normal
live load	0.859	0.150	0.233	extreme type I

4.2. Calculation of Flexural Bearing Capacity Based on Improved Section Method

It is necessary to determine the calculation model for the flexural capacity of the component in three stages, that is, the flexural capacity of the beam at room temperature, the flexural capacity of the beam after fire, the flexural capacity of the beam strengthened with CFRP after fire, as well as related random statistical parameters.

The calculation formula is:

$$M_C = \alpha_1 f_c bx(h_0 - 0.5x) + f_y' A_s'(h_0 - a_s') \tag{22}$$

The concrete in the compression zone of the beam is divided into cells, and the comprehensive temperature of the effective compression zone is calculated as shown in Figure 8.

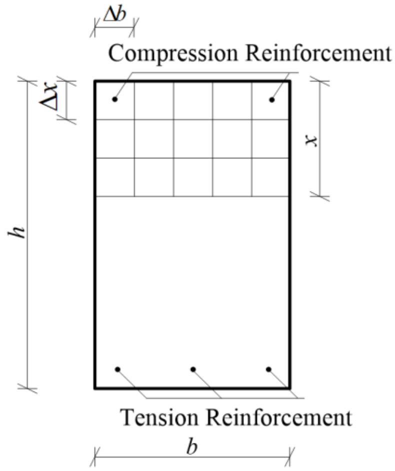

Figure 8: Element division of compression zone after fire.

According to Figure 8 and Equations (19) and (22), the formula for calculating the height of concrete compression zone after fire can be derived as:

$$f_c \sum \overline{\varphi}_{CT_i} \Delta b \Delta x + \varphi_{yT}' f_y' A_s' = \varphi_{yT} f_y A_s \tag{23}$$

Where $\overline{\varphi}_{CT_i}$ is the reduction coefficient of concrete axial compressive strength in i area, which is calculated by the temperature in i area from the finite element simulation.

The reduction coefficient of concrete strength in the compression zone is as follows:

$$\bar{\varphi}_{CT} = \frac{\sum \bar{\varphi}_{CT_i} f_c \Delta b \Delta x}{f_c bx} \tag{24}$$

$$M_{CT} = \alpha_1 \bar{\varphi}_{CT} f_c bx(h-0.5x) + \varphi'_{yT} f'_y A'_s (h-a') - \varphi_{yT} f_y A_s (h-h_0) \tag{25}$$

The bearing capacity of the reinforced beam is:

$$M_D = \alpha_1 \bar{\varphi}_{CT} f_c bx(h-0.5x) + \varphi'_{yT} f'_y A'_s \ h-a') - \varphi_{yT} f_y A_s (h-h_0) - \psi_f f_f A_{fe} (h-0.5x) \tag{26}$$

$$x = (\varphi_{yT} f_y A_S + \psi_f f_f A_{fe} - \varphi'_{yT} f'_y A'_S)/(\alpha_1 \bar{\varphi}_{CT} f_c) \tag{27}$$

Where f_f is average tensile strength, A_{fe} is effective section area, ψ_f is the strength utilization coefficient.

Considering the reinforcement effect of CFRP cannot reach the expected value due to the secondary stress, the strength utilization coefficient of CFRP is:

$$\psi_f = \frac{(0.8\varepsilon_{cu} h/x) - \varepsilon_{cu} - \varepsilon_{fo}}{\varepsilon_f} \qquad x \geq 2a' \tag{28}$$

Where ε_{cu} is ultimate compressive strain of concrete, ε_{fo} is hysteretic strain of CFRP material considering secondary stress effect, ε_f is design value of tensile strain of CFRP.

The probability distribution type of concrete and steel bar strengths is normal distribution, and the detailed statistical parameters of strength random variables are as Table 5 and Table 6. The reinforcing material is single fabric made of CFRP with high strength grade II and its standard tensile strength value is 3000 MPa.

Table 5: Random variables of material strength.

variable	mean value(MPa)	standard value(MPa)	coefficient of variation
compressive strength of C30 concrete	28.03	20.1	0.172
tensile strength of C30 concrete	2.61	2.01	0.14
tensile strength of HRB335 steel	381.64	335	0.0743
compressive strength of HRB335 steel	381.64	335	0.0743
tensile strength of CFRP	3456	3000	0.08

Table 6: Relevant size statistical variables.

variable	Mean value/ standard value	Coefficient of variation
sectional effective height	1.00	0.01
sectional area of longitudinal bar	1.00	0.03
sectional height	1.00	0.01
sectional width	1.00	0.01
sectional area of CFRP	1.00	0.02

4.3. Determination of Limit State Function

The limit state function is established to calculate the structural reliability:

$$Z = R - S = g(X_1, X_2, \ldots X_n) \tag{29}$$

Where R is the resistance of the structure, and S is the effect of the structure.

When calculating the flexural capacity of a beam, the variability of the bearing capacity calculation results is caused by the basic assumptions used in the calculation that do not fully conform to the actual situation or the calculation results are approximate values. Therefore, a random variable γ_m namely the uncertainty coefficient of structural resistance calculation mode is introduced to describe the variation of the bearing capacity calculation result.

$$Z = R - S = \gamma_{\mathrm{m}} M_{\mathrm{C}} - \left(M_{\mathrm{Gm}} + M_{\mathrm{Qm}}\right) \tag{30}$$

Where M_{Gm} is the average value of dead load M_G, M_{Qm} is the average value of live load M_Q.

The limit state function is

$$Z = R - S = \gamma_{\mathrm{m}} M_{CT} - \left(M_{\mathrm{Gm}} + M_{\mathrm{Qm}}\right) \tag{31}$$

Due to the decrease of flexural capacity of reinforced concrete beams after fire, CFRP is used to strengthen the component after fire. The limit state function is:

$$Z = R - S = \gamma_{\mathrm{m}} M_{\mathrm{D}} - \left(M_{\mathrm{Gm}} + M_{\mathrm{Qm}}\right) \tag{32}$$

Load effect ratio n is introduced as

$$n = M_{\mathrm{Qm}} / M_{\mathrm{Gm}} \tag{33}$$

Where the sum of M_{Qm} and M_{Gm} is assumed to be constant. Normally, n is 0.1 to 2.

5. Finite Element Simulation and Calculation for Bearing Capacity

5.1. Load Determination and Load Statistical Parameters

The design dimension of the reinforced concrete beam is 250 mm×600 mm. The concrete type is C30. The beam is reinforced according to the load. The compression and tension reinforcements adopts HRB335, among which three tensile steel bars with diameter of 32 mm and two compressive steel bars with diameter of 22 mm. The stirrup adopts HRB335, with diameter of 8 mm and the stirrup spacing is 150 mm. The distance between the resultant force point of the tensile reinforcement and the edge of the tensile zone, a_s, takes 35 mm. According to the test conditions, the fire on three sides is simulated. Due to the decrease in the bearing capacity of the component after fire, 200 mm-width CFRP sheets with a single layer thickness of 0.167 mm is used to strengthen the component. To reflect reinforcement effect, different layers of CFRP sheets are adhered to the bottom of the beam.

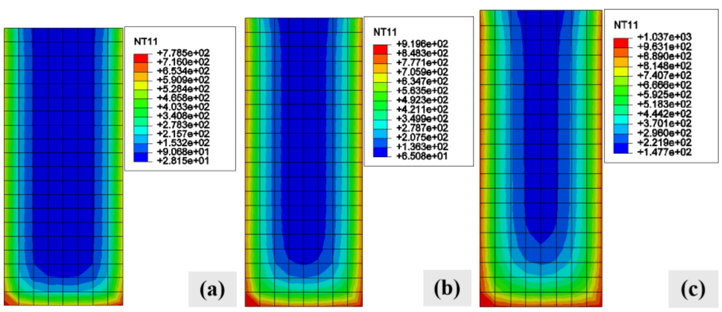

(a) 30min (b) 60min (c) 120min

Figure 9: Temperature nephogram of reinforced concrete beam for different fire time.

The ABAQUS is used to simulate the fire state of RC beams. The tie contact is adopted. The concrete adopts DC3D8 unit with a mesh size of 0.03 m, and the longitudinal reinforcements and stirrups adopt DC1D2 unit with a mesh size of 0.53 m. The temperature field of RC beams subjected to fire for 0.5 h, 1 h and 2 h is simulated according to the actual working conditions, as shown in Figure 9 and Figure 10.

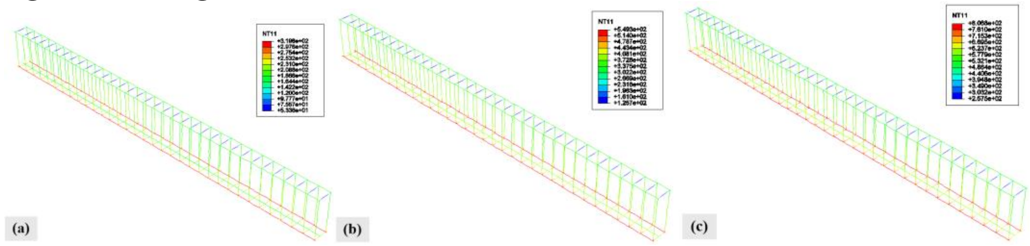

(a) 30min (b) 60min (c) 120min

Figure 10: Temperature nephogram of reinforcements for different fire time.

Temperature distribution of steel bars is the premise for calculating the reduction coefficient of yield strength. The temperature of steel bars after fire is extracted, as shown in Table 7.

Table 7: Reinforcement temperature after fire.

Fire time	Upper rebar(℃)	Lower outer two rebars(℃)	Lower middle rebar(℃)
30 min	190	312	205
60 min	355	545	382
120 min	534	817	612

The temperature distribution diagram of the member after fire is U-shaped. With the increase of fire time, the temperature gradually diffuses from the surface of concrete to the inside of concrete. And the temperature of steel bars also increases gradually. The temperature distribution diagram intuitively shows the trend and change of temperature transmission within the member.

5.2. Reliability Calculation

Based on the strength reduction factor of the compression area under the action of compound temperature, the reliability index of the bearing capacity of the beam under the action of compound temperature is established, and the effects of load effect ratio, fire duration and the number of carbon fiber layers on its bearing capacity are analyzed.

5.2.1. Reliability Calculation of RC Beam at Room Temp

M_{Qm} and M_{Gm} should be determined first, it can be obtained from Equation (21) that M_{sd} =360 $kN \cdot m$, A_s =2413 mm, A_s' =760 mm. Converted from Table 2, it is known that $M_{Qm}+M_{Gm}=28\text{kN}\cdot\text{m}$. Different load effect ratios are selected and the values of M_{Qm} and M_{Gm} under the corresponding load effect ratio are obtained from Equation (32). Combining Equation (22) with Monte Carlo method, MATLAB programming is performed to calculate the reliability index of components with different load effect ratios under room temperature.

5.2.2. Reliability Calculation of RC Beams after Fire

Considering different fire time and load effect ratios, the compression zone height x of concrete corresponding to fire time is obtained through section calculation. The reliability index β is obtained through MATLAB programming based on Equation (30) and Monte Carlo method.

5.2.3. Reliability Calculation of RC Beams Strengthened by CFRP after Fire

The RC beams subjected to fire are strengthened with CFRP, and the corresponding compression zone height x of concrete for different CFRP reinforcement amounts is calculated using Equations (26) and (31). The reliability index of beams under different CFRP reinforcement amounts and different load effect ratios is calculated through MATLAB programming based on Equation (27) and Monte Carlo method.

5.3. Influence of Various Factors on Reliability Index

The finite element models are established to study the reliability index of beams considering factors such as load effect ratio and CFRP reinforcement amount. It is of great significance to understand the changing trends and rules for exploring the safety of reinforced concrete beams strengthened with CFRP after fire. In the parametric analysis, the fire exposure time is 30 minutes, 60 minutes, and 120 minutes, load effect ratio is 0.10, 0.25, 0.50, 0.75 and 1.00, and CFRP layer is 1, 2 and 3 layers, respectively. The corresponding CFRP thicknesses are 0.167 mm, 0.334 mm, and 0.501 mm. The Monte Carlo method is used to program, and 105 cycle simulations are conducted in MATLAB software, the reliability index is shown in Table 8 and Figure 11-Figure 14.

Table 8: Reliability index of flexural bearing capacity.

load effect ratio	unexposed to fire	30 min	60 min	120 min
0.1	3.35	3.21	2.85	2.4
0.25	3.25	3.18	2.76	2.38
0.5	3.10	2.93	2.63	2.24
0.75	2.93	2.75	2.48	2.10
1	2.80	2.62	2.40	2.01

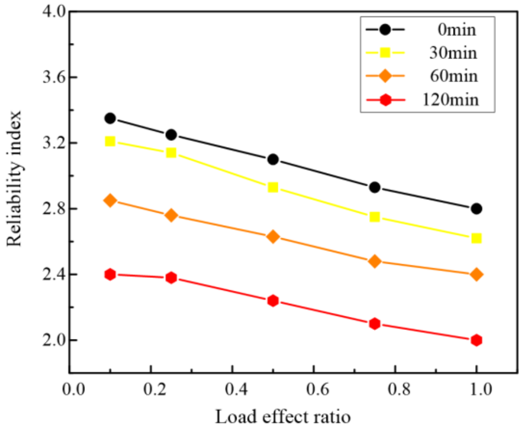

Figure 11: Reliability index with fire time and load effect ratio.

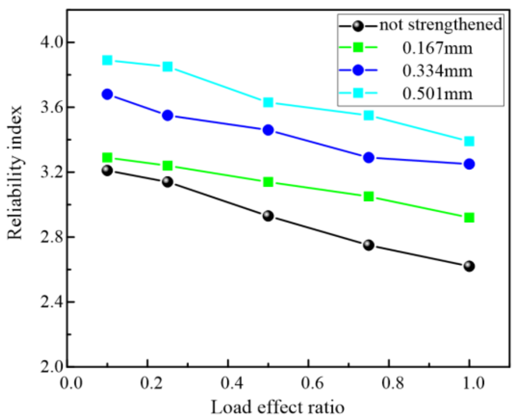

Figure 12: Reliability index with load effect ratio for fire time of 30 minutes.

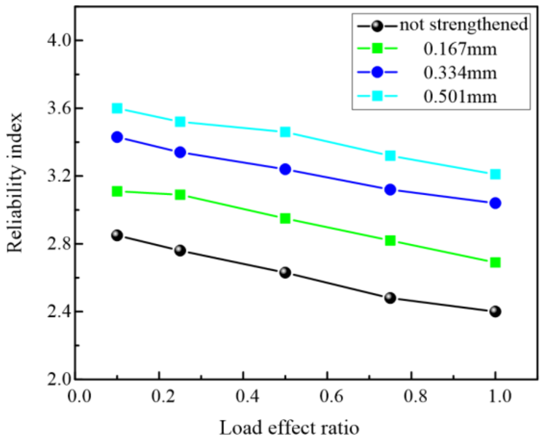

Figure 13: Reliability index with load effect ratio for fire time of 60 minutes.

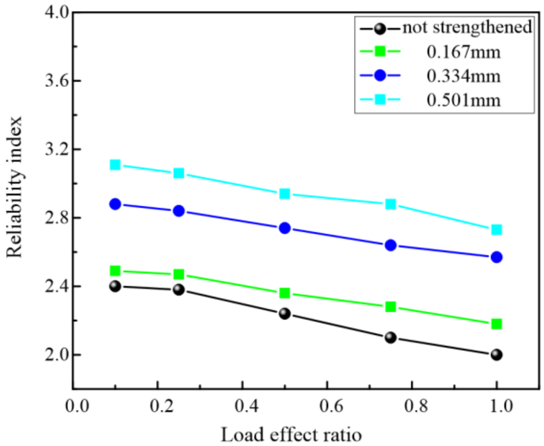

Figure 14: Reliability index with load effect ratio for fire time of 120 minutes.

As can be seen from Figure 11-Figure 14, when the load effect ratio is 1, the reliability index decreases by 6.43% after 30 minutes of fire exposure, 14.29% after 60 minutes, and 28.21% after 120 minutes. When CFRP is used to strengthen the beam after exposure to fire for 30 minutes, the reliability index of the flexural bearing capacity increases by 11.45%, 24.04%, and 29.39% when reinforcing one to three layers, respectively. When the CFRP reinforcement is conducted after 60 minutes exposure to fire, the reliability index increases by 12.08%, 26.67%, and 33.75%, respectively. When the CFRP reinforcement is conducted after 120 minutes exposure to fire, the reliability index increases by 9.00%, 28.50%, and 36.50%, respectively. As the increase of load effect ratio, the variable load also increases. However, since the variable load conforms to the variation distribution of extreme type I, the variability is larger than that of dead load, the reliability index of reinforced concrete beam decreases.

6. Conclusions

Through the collection of fire test data and the integration of finite element simulation results, a set of accurate thermal parameters and finite element simulation calculation method are verified, which will provide valuable experience for the follow-up research on fire. In this paper, the reliability index is used as the unified standard for structural reliability. Moreover, the influences of multiple factors such as different fire time, load effect ratios and the numbers of CFRP reinforced layers on the structural reliability are studied.

(1) The reliability calculation model of residual bearing capacity after fire based on the improved

section method can accurately and effectively evaluate the reliability of flexural bearing capacity of reinforced concrete beams after fire.

(2) Three fire sides are used to simulate the actual fire condition. After 60 minutes of fire, the ultimate bearing capacity of reinforced concrete beams decreases by 27.59% compared with that of non-fire members, so the fire significantly weakens the bearing capacity of reinforced concrete beams.

(3) Reasonable thermal parameters are selected, and finite element simulation software ABAQUS is used to simulate the temperature nephogram of the test beam after fire and the variation of the bearing capacity before and after fire. By comparing the test data with the simulated data, the temperature field error is about 7%, and the flexural bearing capacity error of the beam without fire is 1.2%. The flexural bearing capacity error of the beam subjected to fire for 60 minutes is 2.8%, which proves the correctness of the finite element simulation method and the selection of thermal parameters, and provides theoretical support for the subsequent research.

(4) The reliability index decreases with the increase of load effect ratio and fire time. According to the data, the CFRP-strengthening effect is more obvious with the increase of fire time. By analyzing the strengthening effect of each layer, it can be seen that the reliability index is improved significantly when the first and second layers are strengthened by CFRP, and the reliability index is improved slightly when the third layer is strengthened.

References

[1] Thomaz E. T. B. Analytical and numerical analyses of RC beams exposed to fire adopting a LITS trilinear constitutive law for concrete. Case Studies in Construction Materials. 2022, 17, e01619. https://doi.org/10.1016 / j. c s c m. 2022.e01619.

[2] Roy T., Matsagar, V. A probabilistic framework for assessment of RC wall panel under cascaded post blast fire scenario. Journal of Building Engineering. 2022, 45, 103506. https://doi.org / 10.1016/j. job e. 2021.103506.

[3] Melo, J., Zafiris, T., David, R., et al. Cyclic behavior of as built and strengthened existing RC columns previously damaged by fire. Engineering Structures. 2022, 266, 114584. https://doi.org/10.1016/j.engstruct. 2 022.114584.

[4] XU YY, WU, B., WAN, R. H. Experimental study on residual performance of RC beam s after fire. Journal of Building Structure s. 2013, 34, 20-29. doi:10.14006/j.jzjgxb.2013.08.004.

[5] LI, Y. Z., TANG, Y. J., XU, Z. S. Experimental Study on Bearing Capacity and Reliability Analysis of Reinforced Concrete Simple Support Beam after Fire Damage. China Safety Science Journal. 2004, 10, 88-92+3. DOI:10.16265/j.cnki.issn1003-3033.2004.10.020.

[6] Yaroslav, B., Jacek, S., Rostyslav, V., et al. Strengthening Reinforced Concrete eccentrically loaded columns by CFRP at different levels of initial load. Engineering Structures. 2023, 280, 115694. https://doi. org/10.1016/j.eng struct.2023.115694.

[7] Azeedo, A.S., Frmo, J.P., Coreia, J.R., et al. Fire behaviour of C F R P strengthened Reinforced Concrete slabs using different techniques-EBR, NSM and Create. Composites Part B: Engineering. 2022, 230, 109471. https://doi.org/10.1016/j. composite sb. 2021.109471.

[8] Muazzam, G. S., Muhammad, W., Nasser, A. N., et al. Behavior of artificially corroded reinforced Concrete beams strengthened with CFRP and hybrid CFRP-GFRP laminates. Engineering Structures. 2016, 272, 114827. https://doi.org/10.1016/j. engstruct. 2022.114827.

[9] Zhu, C. Q., Zhang, D. B., Zhu, H. Y. Reliability Analysis on Bolt Support Structure of Coal Roadway Based on Monte-Carlo. China Safety Science Journal. 2008, 04, 146-150. DOI:10.16265/j.cnki.issn1003-3033.2008.04.003.

[10] European Committee for Standardization, ENV 1994-1-2, Eurocode 4, Design of Composite and Concrete Structures, part1.2: Structural Fire Design, 1994.

[11] Lie, T. T., De ham, E. M. A. Factors affecting the fire resistance of circular hollow steel columns filled with bar RC. N R C- C NRC Internal Report. 1993, 651, 103506.

[12] European Committe for Standardization, ENV 1993-1- 2, Eurocode 3, Design of Steel Structures, part1.2: Structural Fire Design, 1993.

[13] Lie, T. T., Irwn, R. J. Fire resistance of rectangular steel columns filled with reinforced Concrete. Journal of Structural Engineering.1995, 121(5) : 797-805

[14] Lu, Z. D., Chai, L. F., Yu, J. E. Calculation and analysis of mechanical properties of reinforced concrete continuous beam after fire. Journal of Tongji University (Natural Science). 2015, 43, 16-26. https:// k ns.cnki.net/ k

cms/ detail/ 10.11908/ j. is sn. 0253-374x. 2015.01. 003. html
[15] Gernay, T., Milard, A., Fransen, J. M. A Multiaxial Constitutive Model for RC in the Fire Situation: Theoretical Formulation. International Journal of Solids and Structures. 2013, 50, 3659-3673. https:// doi.org/10.10 16 /j.ijsolstr. 2013.07.013.
[16] Ministry of Houing and Urban-Rural Construction of the People's Republic of China. Unified Standard for Reliability Design of Engineering Structures (G B 50153-2008). Beijing: China Architecture and Building Press, 2008.
[17] Roy, T., Vasant, M. Evaluation of rebar mechanical properties after high temp (Fire Exposure). Sichuan Building Science. 1991, 02, 05-09.